Inorg. Chem. **2007**, *46*, 6011–6021

Marked Differences in Light-Switch Behavior of Ru(II) Complexes Possessing a Tridentate DNA Intercalating Ligand

Yao Liu,[†] Richard Hammitt,[‡] Daniel A. Lutterman,[†] Randolph P. Thummel,*[,‡] and Claudia Turro*[,†]

Department of Chemistry, The Ohio State University, Columbus, Ohio 43210, and Department of Chemistry, University of Houston, Houston, Texas 77204

Received March 13, 2007

The tridentate ligand 3-(pyrid-2′-yl)dipyrido[3,2-*a*:2′,3′-*c*]phenazine (pydppz) has been prepared in two steps by elaboration of 2-(pyrid-2′-yl)-1,10-phenanthroline. Both homoleptic $[Ru(pydppz)_2]^{2+}$ and heteroleptic $[Ru(tpy)(pydppz)]^{2+}$ (tpy = 2,2′;6′,2″-terpyridine) complexes have been prepared and characterized by ^{1}H NMR. The absorption and emission spectra are consistent with low-lying MLCT excited states, which are typical of Ru(II) complexes. Femtosecond transient absorption measurements show that that the ^{3}MLCT excited state of the heteroleptic complex $[Ru(tpy)(pydppz)]^{2+}$ ($\tau \approx 5$ ns) is longer-lived than that of the homoleptic complex $[Ru(pydppz)_2]^{2+}$ ($\tau = 2.4$ ns) and that these lifetimes are significantly longer than that of the ^{3}MLCT state of the parent complex $[Ru(tpy)_2]^{2+}$ ($\tau =$ 120 ps). These differences are explained by the lower-energy ^{3}MLCT excited state present in $[Ru(tpy)(pydppz)]^{2+}$ and $[Ru(pydppz)_2]^{2+}$ compared to $[Ru(tpy)_2]^{2+}$, resulting in less deactivation of the former through the ligand-field state(s). DFT and TDDFT calculations are consistent with this explanation. $[Ru(tpy)(pydppz)]^{2+}$ and $[Ru(pydppz)_2]^{2+}$ bind to DNA through the intercalation of the pydppz ligand; however, only the heteroleptic complex exhibits luminescence enhancement in the presence of DNA. The difference in the photophysical behavior of the complexes is explained by the inability of $[Ru(pydppz)_2]^{2+}$ to intercalate both pydppz ligands, such that one pydppz always remains exposed to the solvent. DNA photocleavage is observed for $[Ru(tpy)(pydppz)]^{2+}$ in air, but not for $[Ru(pydppz)_2]^{2+}$. The DNA damage likely proceeds through the production of small amounts of $^1O_2$ by the longer-lived complex. Although both complexes possess the intercalating pydppz ligand, they exhibit different photophysical properties in the presence of DNA.

Introduction

Ru(II) complexes with planar polycyclic aromatic ligands are potentially useful in biotechnology applications owing to their DNA binding through intercalation and associated emission enhancement.[1−6] Luminescent Ru(II) complexes that interact with nucleic acids have been used in the quantitative detection of DNA,[7,8] DNA hybridization,[9−12] mismatch detection,[10,13−15] DNA−drug interactions,[16,17] and electronics.[18,19] However, the need still remains for new

* To whom correspondence should be addressed. E-mail: turro@chemistry.ohio-state.edu (C.T.), thummel@uh.edu (R.P.T.).
[†] The Ohio State University.
[‡] University of Houston.

(1) (a) Gorodetsky, A. A.; Barton, J. K. *Langmuir* **2006**, *22*, 7917−7922. (b) Drummond, T. G.; Hill, M. G.; Barton, J. K. *Nat. Biotechnol.* **2003**, *21*, 1192−1199. (c) Erkkila, K. E.; Odom, D. T.; Barton, J. K. *Chem. Rev.* **1999**, *99*, 2777−2795.
(2) Elias, B.; Kirsch-De Mesmaeker, A. *Coord. Chem. Rev.* **2006**, *250*, 1627−1641.
(3) Metcalfe, C.; Thomas, J. A. *Chem. Soc. Rev.* **2003**, *32*, 215−224.
(4) Xie, H.; Tansil, N. C.; Gao, Z. *Front. Biosci.* **2006**, *11*, 1147−1157.
(5) Nordell, P.; Lincoln, P. *J. Am. Chem. Soc.* **2005**, *127*, 9670−9671.
(6) Koehne, J. E.; Chen, H.; Cassell, A. M.; Qi, Y.; Han, J.; Meyyappan, M.; Li, J. *Clin. Chem.* **2004**, *50*, 1886−1893.
(7) Cao, W.; Ferrance, J. P.; Demas, J.; Landers, J. P. *J. Am. Chem. Soc.* **2006**, *128*, 7572−7578.
(8) Li, C.; Liu, S.; Guo, L.-H.; Chen, D. *Electrochem. Commun.* **2005**, *7*, 23−28.
(9) Kitamura, Y.; Ihara, T.; Okada, K.; Tsujimura, Y.; Shirasaka, Y.; Tazaki, M.; Jyo, A. *Chem. Comm.* **2005**, 4523−4525.
(10) Spehar-Deleze, A.-M.; Schmidt, L.; Neier, R.; Kulmala, S.; de Rooij, N.; Koudelka-Hep, M. *Biosensors Bioelectronics* **2006**, *22*, 722−729.
(11) Liu, S.; Li, C.; Cheng, J.; Zhou, Y. *Anal. Chem.* **2006**, *78*, 4722−4726.
(12) Firrao, G. *Int. J. Environm. Anal. Chem.* **2005**, *85*, 609−612.
(13) (a) Boon, E. M.; Kisko, J. L.; Barton, J. K. *Methods Enzymol.* **2002**, *353*, 506−522. (b) Rueba, E.; Hart, J. R.; Barton, J. K. *Inorg. Chem.* **2004**, *43*, 4570−4578.
(14) Bichenkova, E. V.; Yu, X.; Bhadra, P.; Heissigerova, H.; Pope, S. J. A.; Coe, B. J.; Faulkner, S.; Douglas, K. T. *Inorg. Chem.* **2005**, *44*, 4112−4114.
(15) Yu, C. J.; Wan, Y.; Yowanto, H.; Li, J.; Tao, C.; James, M. D.; Tan, C. L.; Blackburn, G. F.; Meade, T. J. *J. Am. Chem. Soc.* **2001**, *123*, 11155−11161.

10.1021/ic700484j CCC: $37.00
Published on Web 06/14/2007

complexes with improved properties, such as better detection limits and selectivity. To this end, numerous complexes with ligands that are able to intercalate between the DNA bases have been designed, many of which are derived from the parent complex $[Ru(bpy)_3]^{2+}$ (bpy = 2,2′-bipyridine). Some examples are complexes of the type $[Ru(bpy)_2(L)]^{2+}$, where the intercalating ligand L includes dipyrido[3,2-*f*:2′,3′-*h*]-quinoxaline (dpq),[20,21] dipyrido[3,2-*a*:2′,3′-*c*]phenazine (dppz),[22,23] tetrapyrido[3,2-*a*:2′,3′-*c*:3″,2″-*h*:2‴,3‴-*j*]phenazine (tpphz),[24,25] benzo[*i*]dipyrido[3,2-*a*:2′,3′-*c*]phenazine (dppn),[21,26] naphtho[2,3-*f*][*1*,*ω*]phenanthroline,[27] eilatin,[28−30] and 1,12-diazaperylene (DAP).[31] In general, the binding of these complexes to DNA greatly affects their luminescence.

In contrast to $[Ru(bpy)_3]^{2+}$, $[Ru(tpy)_2]^{2+}$ (tpy = 2,2′;6′,2″-terpyridine) exhibits weak emission and a short-lived excited state at room temperature, making it less useful for biological applications.[32−36] It has been shown, however, that the luminescence intensity and lifetime of complexes derived from $[Ru(tpy)_2]^{2+}$ can be increased significantly through modification of the tpy ligand with various groups.[37−41] In addition, Ru(II) complexes possessing tridentate ligands related to tpy have also been shown to exhibit extended emission lifetimes compared to $[Ru(tpy)_2]^{2+}$.[42] Although the lifetimes of the ^{3}MLCT (metal-to-ligand charge transfer) excited states of these complexes remain relatively short compared to systems derived from $[Ru(bpy)_3]^{2+}$, the ^{3}MLCT excited state in some of these Ru(II)−tpy systems is still able to sensitize enough $^1O_2$ to effect DNA photocleavage.[43]

Modified tpy ligands have been shown to act as robust bridging ligands for the generation of multimetallic structures,[44−46] or have served as terminal ligands in supramolecular architectures.[47,48] In other systems, substituted tpy ligands were used to juxtapose various electron donors and acceptors, generating diads and triads.[49−51] The multimetallic complexes and the donor−acceptor systems may have applications in solar energy conversion arrays.[52,53] Other Ru(II) complexes with substituted tpy ligands have been shown to act as pH sensors,[54] to exhibit temperature-dependent dual emission,[55] to act as prototypes for molecular machines,[56] and were used as building blocks in the generation of metal-containing dendrimers and polymers.[57,58] Bimetallic complexes of the type (tpy)Ru(tpy)−(BL)−$PtCl_2$, where BL =

(16) Bagni, G.; Ravera, M.; Osella, D.; Mascini, M. *Curr. Pharm. Anal.* **2005**, *1*, 217−224.
(17) Kuwabara, T.; Noda, T.; Ohtake, H.; Ohtake, T.; Toyama, S.; Ikariyama, Y. *Anal. Biochem.* **2003**, *314*, 30−37.
(18) Wilhelmsson, L. M.; Westerlund, F.; Lincoln, P.; Norden, B. *J. Am. Chem. Soc.* **2002**, *124*, 12092−12093.
(19) Napier, M. E.; Hull, D. O.; Thorp, H. H. *J. Am. Chem. Soc.* **2005**, *127*, 11952−11953.
(20) (a) Collins, J. G.; Aldrich-Wright, J. R.; Greguric, I. D.; Pellegrini, P. A. *Inorg. Chem.* **1999**, *38*, 5502−5509. (b) Greguric, I.; Aldrich-Wright, J. R.; Collins, J. G. *J. Am. Chem. Soc.* **1997**, *119*, 3621−3622.
(21) O'Donoghue, K.; Penedo, J. C.; Kelly, J. M.; Kruger, P. E. *Dalton Trans.* **2005**, 1123−1128.
(22) (a) Hartshorn, R. M.; Barton, J. K. *J. Am. Chem. Soc.* **1992**, *114*, 5919−5925. (b) Jenkins, Y.; Barton, J. K. *J. Am. Chem. Soc.* **1992**, *114*, 8736−8738. (c) Jenkins, Y.; Friedman, A. E.; Turro, N. J.; Barton, J. K. *Biochemistry* **1992**, *31*, 10809−10816. (d) Friedman, A. E.; Chambron, J. C.; Sauvage, J. P.; Turro, N. J.; Barton, J. K. *J. Am. Chem. Soc.* **1990**, *112*, 4960−4962.
(23) Hiort, C.; Lincoln, P.; Norden, B. *J. Am. Chem. Soc.* **1993**, *115*, 3448−3454.
(24) Liu, Y.; Chouai, A.; Degtyareva, N. N.; Lutterman, D. A.; Dunbar, K. R.; Turro, C. *J. Am. Chem. Soc.* **2005**, *127*, 10796−10797.
(25) Tysoe, S. A.; Kopelman, R.; Schelzig, D. *Inorg. Chem.* **1999**, *38*, 5196−5197.
(26) Lo, K. K.-W.; Chung, C.-K.; Zhu, N. *Chem. Eur. J.* **2006**, *12*, 1500−1512.
(27) Albano, G.; Belser, P.; De Cola, L.; Gandolfi, M. T. *Chem. Commun.* **1999**, 1171−1172.
(28) Bergman, S. D.; Gut, D.; Kol, M.; Sabatini, C.; Barbieri, A.; Barigelletti, F. *Inorg. Chem.* **2005**, *44*, 7943−7950.
(29) Kirk, S. R.; Luedtke, N. W.; Tor, Y. *Bioorg. Med. Chem.* **2001**, *9*, 2295−2301.
(30) (a) Luedtke, N. W.; Hwang, J. S.; Nava, E.; Gut, D.; Kol, M.; Tor, Y. *Nucl. Acids Res.* **2003**, *31*, 5732−5740. (b) Luedtke, N. W.; Tor, Y. *Biopolymers* **2003**, *70*, 103−119.
(31) Chouai, A.; Wicke, S. E.; Turro, C.; Bacsa, J.; Dunbar, K. R.; Wang, D.; Thummel, R. P. *Inorg. Chem.* **2005**, *44*, 5996−6003.
(32) Carter, P. J.; Cheng, C.-C.; Thorp, H. H. *J. Am. Chem. Soc.* **1998**, *120*, 632−642.
(33) Ossipov, D.; Gohil, S.; Chattopadhyaya, J. *J. Am. Chem. Soc.* **2002**, *124*, 13416−13433.
(34) van der Schilden, K.; Garcia, F.; Kooijman, H.; Spek, A. L.; Haasnoot, J. G.; Reedijk, J. *Angew. Chem., Int. Ed.* **2004**, *43*, 5668−5670.
(35) Ding, H.-Y.; Wang, X.-S.; Song, L.-Q.; Chen, J.-R.; Yu, J.-H.; Chao, L.; Zhang, B.-W. *J. Photochem. Photobiol. A* **2006**, *177*, 286−294.
(36) Chao, H.; Mei, W.-J.; Huang, Q.-W.; Ji, L.-N. *J. Inorg. Biochem.* **2002**, *92*, 165−170.
(37) Hecker, C. R.; Gushurst, A. K. I.; McMillin, D. R. *Inorg. Chem.* **1991**, *30*, 538−41.
(38) Polson, M. I. J.; Medlycott, E. A.; Hanan, G. S.; Mikelsons, L.; Taylor, N. J.; Watanabe, M.; Tanaka, Y.; Loiseau, F.; Passalacqua, R.; Campagna, S. *Chem. Eur. J.* **2004**, *10*, 3640−3648.
(39) Abrahamsson, M.; Wolpher, H.; Johansson, O.; Larsson, J.; Kritikos, M.; Eriksson, L.; Norrby, P.-O.; Bergquist, J.; Sun, L.; Akermark, B.; Hammarstrom, L. *Inorg. Chem.* **2005**, *44*, 3215−25.
(40) Duati, M.; Tasca, S.; Lynch, F. C.; Bohlen, H.; Vos, J. G.; Stagni, S.; Ward, M. D. *Inorg. Chem.* **2003**, *42*, 8377−8384.
(41) Maestri, M.; Armaroli, N.; Balzani, V.; Constable, E. C.; Thompson, A. M. W. C. *Inorg. Chem.* **1995**, *34*, 2759−2767.
(42) Abrahamsson, M.; Jager, M.; Osterman, T.; Eriksson, L.; Persson, P.; Becker, H.-C.; Johansson, O.; Hammarstrom, L. *J. Am. Chem. Soc.* **2006**, *128*, 12616−12617.
(43) Ding, H.-Y.; Wang, X.-S.; Song, L.-Q.; Chen, J.-R.; Yu, J.-H.; Chao, L.; Zhang, B.-W. *Photochem. Photobiol. A* **2006**, *177*, 286−294.
(44) Gagliardo, M.; Rodriguez, G.; Dam, H. H.; Lutz Martin, S.; Anthony, L.; Havenith, R. W. A.; Coppo, P.; De Cola Luisa, H.; Frantisek Van Klink, G. P. M.; van Koten, G. *Inorg. Chem.* **2006**, *45*, 2143−2155.
(45) (a) Stadler, A.-M.; Puntoriero, F.; Campagna, S.; Kyritsakas, N.; Welter, R.; Lehn, J.-.M. *Chem. Eur. J.* **2005**, *11*, 3997−4009. (b) Ceroni, P.; Credi, A.; Balzani, V.; Campagna, S.; Hanan, G. S.; Arana, C. R.; Lehn, J.-M. *Eur. J. Inorg. Chem.* **1999**, *9*, 1409−1414. (c) Hasenknopf, B.; Hall, J.; Lehn, J.-M.; Balzani, V.; Credi, A.; Campagna, S. *New J. Chem.* **1996**, *20*, 725−730.
(46) Indelli, M. T.; Scandola, F.; Flamigni, L.; Collin, J.-P.; Sauvage, J.-P.; Sour, A. *Inorg. Chem.* **1997**, *36*, 4247−4250.
(47) (a) Harriman, A.; Mayeux, A.; Stroh, C.; Ziessel, R. *Dalton Trans.* **2005**, 2925−2932. (b) Harriman, A.; Mayeux, A.; De Nicola, A.; Ziessel, R. *Phys. Chem. Chem. Phys.* **2002**, *4*, 2229−2235.
(48) Swavey, S.; Fang, Z.; Brewer, K. J. *Inorg. Chem.* **2002**, *41*, 2598−2607.
(49) Collin, J. P.; Guillerez, S.; Sauvage, J. P.; Barigelletti, F.; De Cola, L.; Flamigni, L.; Balzani, V. *Inorg. Chem.* **1991**, *30*, 4230−8.
(50) Laine, P.; Bedioui, F.; Amouyal, E.; Albin, V.; Berruyer-Penaud, F. *Chem. Eur. J.* **2002**, *8*, 3162−3176.
(51) Benniston, A. C.; Chapman, G. M.; Harriman, A.; Rostron, S. A. *Inorg. Chem.* **2005**, *44*, 4029−4036.
(52) Medlycott, E. A.; Hanan, G. S. *Chem. Soc. Rev.* **2005**, *34*, 133−142.
(53) (a) Baranoff, E.; Collin, J.-P.; Flamigni, L.; Sauvage, J.-P. *Chem. Soc. Rev.* **2004**, *33*, 147−155. (b) Flamigni, L.; Barigelletti, F.; Armaroli, N.; Collin, J.-P.; Dixon, I. M.; Sauvage, J.-P.; Williams, J. A. G. *Coord. Chem. Rev.* **1999**, *190−192*, 671−682.
(54) Constable, E. C.; Housecroft, C. E.; Thompson, A. C.; Passaniti, P.; Silvi, S.; Maestri, M.; Credi, A. *Inorg. Chim. Acta* **2007**, *360*, 1102−1110.
(55) Wang, J.; Medlycott, E. A.; Hanan, G. S.; Loiseau, F.; Campagna, S. *Inorg. Chim. Acta* **2007**, *360*, 876−884.
(56) Bonnet, S.; Collin, J.-P.; Koizumi, M.; Mobian, P.; Sauvage, J.-P. *Adv. Mater.* **2006**, *18*, 1239−1250.
(57) Cho, T. J.; Moorefield, C. N.; Wang, P.; Newkome, G. R. *ACS Symp. Ser.* **2006**, *928*, 186−204.

bridging ligand, have been shown to bind covalently to DNA through the Pt(II) center, while the related (tpy)ClRu(BL)-$RhCl_2$ complexes are able to photocleave DNA.[59] Complexes of the type $[Ru(tpy)(bpy)O]^{2+}$ are able to oxidatively cleave RNA and DNA,[60] and this short-range DNA scission has been used to determine the intercalation sites of the related complex $[Ru(tpy)(dppz)O]^{2+}$.[61]

The present work focuses on the synthesis of complexes related to $[Ru(tpy)_2]^{2+}$ that involve a new tridentate intercalating ligand, pydppz (pydppz = 3-(pyrid-2′-yl)dipyrido-[3,2-*a*:2′,3′-*c*]phenazine). Unlike the previously studied DNA intercalating complexes $[Ru(bpy)_2L]^{2+}$ which are tris-bidentate, these new complexes are bis-tridentate. Rather than having three planar bidentate ligands orthogonally arranged around the metal center, the pydppz complexes have only two mutually perpendicular tridentate ligands and thus possess a more "open" structure which could have important implications in DNA binding. The series $[Ru(tpy)_n(pydppz)_{2-n}]^{2+}$ ($n = 0, 1, 2$) was prepared and characterized, and photophysical properties, electrochemistry, and DNA binding were investigated. The results show a marked difference in photophysical behavior between $[Ru(tpy)(pydppz)]^{2+}$ and $[Ru(pydppz)_2]^{2+}$ when bound to DNA. This observation is unusual, since both complexes possess the intercalating pydppz ligand. The difference in light-switch behavior is explained by the unique electronic structure of each complex.

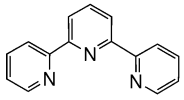

tpy

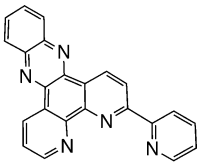

pydppz

Experimental Section

Materials. Sodium chloride, sodium phosphate, gel loading buffer (0.05% (w/v) bromophenol blue, 40% (w/v) sucrose, 0.1 M ethylenediaminetetraacetic acid (EDTA) (pH 8.0), 0.5% (w/v) sodium lauryl sulfate), tris(hydroxymethyl)aminomethane (Tris base), Tris/HCl, and ethidium bromide were purchased from Sigma and used as received. Calf thymus DNA was purchased from Sigma and was dialyzed against a 5 mM Tris, 50 mM NaCl (pH 7.5) buffer three times during a 48 h period prior to use. The relative absorption of the resulting solution at 260 and 280 nm ($A_{260}/A_{280} \geq 1.8$) was used to monitor the purity of the sample. The pUC18 plasmid was purchased from Bayou Biolabs and purified using the Concert Miniprep System from Life Technology. Acetonitrile was dried over CaH_2 and distilled under an argon atmosphere prior to use. $RuCl_3 \cdot 3H_2O$, KBr, *o*-phenylenediamine, 2,2′;6′,2″-terpyridine, and NH_4PF_6 were commercially available. $[Ru(tpy)Cl_3]$,[62] $[Ru(tpy)_2]^{2+}$,[63] and 2-(pyrid-2′-yl)-1,10-phenanthroline were prepared by methods previously reported.[64] The microwave reactions were carried out in a household microwave oven modified according to a published description.[65]

2-(Pyrid-2′-yl)-1,10-phenanthroline-5,6-dione (2). KBr (0.69 g, 5.8 mmol) was added to 2-(pyrid-2′-yl)-1,10-phenanthroline (0.15 g, 0.58 mmol) at 0 °C. H_2SO_4 (2 mL) and HNO_3 (1 mL), previously cooled to 0 °C, was added dropwise. The suspension was heated to 88 °C and stirred for 20 h. The solution was cooled to 25 °C and neutralized with $NaHCO_3$. The suspension was filtered, and the filtrate was extracted with CH_2Cl_2 (3 × 75 mL). The combined organic phases were dried over $MgSO_4$ and concentrated. The residue was purified by chromatography on SiO_2 (10 g), eluting with $MeOH/CH_2Cl_2$ (1:10) to obtain **2** (0.13 g, 78%) as yellow flakes: mp > 280 °C; ^{1}H NMR ($CDCl_3$) δ 9.18 (dd, 1 H, $J = 1.8$, 4.8 Hz), 8.83 (dt, 1 H, $J = 1.2$, 7.8 Hz), 8.78 (ddd, 1 H, $J = 0.6$, 1.8, 4.8 Hz), 8.74 (d, 1 H, $J = 8.4$ Hz), 8.64 (d, 1 H, $J = 1.8$, 7.8 Hz), 8.54 (dd, 1 H, $J = 1.8$, 7.8 Hz), 7.95 (td, 1 H, $J = 1.2$, 7.8 Hz), 7.62 (dd, 1 H, $J = 4.8$, 7.8 Hz), 7.42 (ddd, 1 H, $J = 1.2$, 4.8, 7.2 Hz); ^{13}C NMR could not be obtained due to poor solubility; IR 1678 cm^{-1}. Anal. Calcd for $C_{17}H_9N_3O_2 \cdot 0.25H_2O$: C, 69.98; H, 3.15; N, 14.41. Found: C, 69.81; H, 2.89; N, 14.39.

3-(Pyrid-2′-yl)dipyrido[3,2-*a*:2′,3′-*c*]phenazine (3, pydppz). EtOH (15 mL) was added to *o*-phenylenediamine (97 mg, 0.90 mmol) and **2** (100 mg, 0.34 mmol). The suspension was heated to reflux and stirred under Ar for 2 h. The suspension was filtered, and the solid was washed with EtOH and acetone. The solid was dried under vacuum to provide pydppz (0.123 g, 98%) as white flakes: mp 282−284 °C; ^{1}H NMR ($CDCl_3$) δ 9.74 (d, 1 H, $J =$ 8.7 Hz), 9.68 (dd, 1 H, $J = 1.5$, 7.8 Hz), 9.34 (dd, 1 H, $J = 1.5$, 4.5 Hz), 9.02 (d, 1 H, $J = 7.5$ Hz), 8.95 (d, 1 H, $J = 9.3$ Hz), 8.79 (dd, 1 H, $J = 1.2$, 3.9 Hz), 8.35 (m, 2 H), 7.97 (dt, 1 H, $J = 1.8$, 7.8 Hz), 7.91 (m, 2 H), 7.82 (dd, 1 H, $J = 4.5$, 8.4 Hz), 7.42 (ddd, 1 H, $J = 1.2$, 4.8, 7.5 Hz); ^{13}C NMR ($CDCl_3$) δ 158.5, 155.8, 152.7, 149.3, 147.9, 142.7, 142.5, 141.3, 141.2, 137.2, 134.9, 134.0, 130.8, 130.7, 129.7, 129.6, 127.9, 127.7, 124.6, 124.1, 123.0, 122.8, 121.8. Anal. Calcd for $C_{23}H_{13}N_5 \cdot 0.5H_2O$: C, 75.00; H, 3.80; N, 19.02. Found: C, 74.85; H, 3.65; N, 18.79.

[Ru(tpy)(pydppz)](PF$_6$)$_2$. EtOH (10 mL) and water (10 mL) were added to pydppz (83 mg, 0.23 mmol) and $[Ru(tpy)Cl_3]$ (68 mg, 0.15 mmol). The suspension was stirred at reflux under Ar for 21 h. The EtOH was evaporated and the solution was added dropwise to a solution of NH_4PF_6 (200 mg, 1.20 mmol) in water (5 mL). The precipitate was filtered and washed with ether. The solid was purified by chromatography on silica, eluting with CH_3CN/1 M $NaNO_3$ (4:1). Precipitation using NH_4PF_6 provided $[Ru(tpy)(pydppz)](PF_6)_2$ (120 mg, 80%) as a red solid: mp > 300 °C; ^{1}H NMR (CD_3CN) δ 9.78 (d, 1 H, $J = 8.4$ Hz), 9.44 (dd, 1 H, $J = 0.6$, 7.5 Hz), 9.13 (d, 1 H, $J = 9.3$ Hz), 8.80 (d, 2 H, $J = 8.1$ Hz), 8.67 (d, 1 H, $J = 7.8$ Hz), 8.53 (m, 5 H), 8.17 (m, 2 H), 7.99 (dt, 1 H, $J = 0.9$, 7.5 Hz), 7.89 (dt, 2 H, $J = 1.2$, 7.8 Hz), 7.77 (dd, 1 H, $J = 1.8$, 5.1 Hz), 7.61 (dd, 1 H, $J = 6.0$, 8.1 Hz), 7.50 (d, 1 H, $J = 4.8$ Hz), 7.34 (d, 2 H, $J = 5.4$ Hz), 7.22 (ddd, 1 H, $J = 1.2$, 5.4, 6.6 Hz), 7.05 (ddd, 2 H, $J = 1.2$, 5.4, 6.0 Hz). Anal.

(58) (a) Andres, P. R.; Schubert, U. S. *Adv. Mat.* **2004**, *16*, 1043−1068. (b) Schubert, U. S.; Eschbaumer, C. *Angew. Chem., Int. Ed.* **2002**, *41*, 2892−2926.
(59) (a) Holder, A. A.; Swavey, S.; Brewer, K. J. *Inorg. Chem.* **2004**, *43*, 303−308. (b) Williams, R. L.; Toft, H. N.; Winkel, B.; Brewer, K. J. *Inorg. Chem.* **2003**, *42*, 4394−4400. (c) Fang, Z.; Swavey, S.; Holder, A.; Winkel, B.; Brewer, K. J. *Inorg. Chem. Comm.* **2002**, *5*, 1078−1081.
(60) (a) Farrer, B. T.; Thorp, H. H. *Inorg. Chem.* **2000**, *39*, 44−49. (b) Yang, I. V.; Thorp, H. H. *Inorg. Chem.* **2001**, *40*, 1690−1697.
(61) Carter, P. J.; Cheng, C.-C.; Thorp, H. H. *J. Am. Chem. Soc.* **1998**, *120*, 632−642.
(62) Schubert, U. S.; Eschbaumer, C.; Andres, P.; Hofmeier, H.; Weidl, C. H.; Herdtweck, E.; Dulkeith, E.; Morteani, A.; Hecker, N. E.; Feldmann, J. *Synth. Met.* **2001**, *121*, 1249−1252.
(63) Braddoc, J. N.; Myer, T. J. *J. Am. Chem. Soc.* **1973**, *10*, 3158.
(64) Hung, C.; Wang, T.; Shi, Z.; Thummel, R. P. *Tetrahedron* **1994**, *50*, 10685−10692.
(65) Matsumura-Inoue, T.; Tanabe, M.; Minami, T.; Ohashi, T. *Chem. Lett.* **1994**, 2443−2446.

Calcd for $C_{38}H_{24}N_8RuP_2F_{12}\cdot 0.5H_2O$: C, 45.98; H, 2.54; N, 11.29. Found: C, 46.29; H, 2.66; N, 10.77.

[Ru(pydppz)$_2$](PF$_6$)$_2$. $RuCl_3\cdot 3H_2O$ (10.7 mg, 0.051 mmol) and ethylene glycol (2.5 mL) were added to pydppz (37 mg, 0.10 mmol). The suspension was heated in a microwave oven for 30 min. The suspension was then added to NH_4PF_6 (34 mg, 0.20 mmol) in water (10 mL). The precipitate was filtered and washed with EtOH and ether. The solid was then purified by chromatography on alumina (15 g). Eluting with CH_3CN/CH_2Cl_2 (2:1) provided $[Ru(pydppz)_2](PF_6)_2$ (54 mg, 95%) as a red powder: ^{1}H NMR (CD_3CN) δ 9.88 (d, 1 H, J = 8.7 Hz), 9.45 (dd, 1 H, J = 1.2, 7.8 Hz), 9.22 (d, 1 H, J = 9.0 Hz), 8.74 (d, 1 H, J = 8.1 Hz), 8.60 (m, 1 H), 8.48 (m, 1 H), 8.20 (m, 2 H), 8.00 (td, 1 H, J = 1.2, 7.5 Hz), 7.79 (dd, 1 H, J = 1.2, 5.4 Hz), 7.54 (dd, 1 H, J = 5.7, 8.4 Hz), 7.53 (d, 1 H, J = 5.4 Hz), 7.15, (ddd, 1 H, J = 0.9, 5.4, 7.5 Hz); MS (ESI) m/z 964 ($M^+ - 143$), 411 ($M^{2+} - 290$)/2. Anal. Calcd for $C_{46}H_{26}N_{10}RuP_2F_{12}\cdot 3H_2O$: C, 47.49; H, 2.77; N, 12.04. Found: C, 47.66; H, 2.90; N, 11.88.

Instrumentation. ^{1}H NMR spectra were obtained at 300 MHz and ^{13}C NMR spectra were obtained at 75 MHz on a General Electric QE-300 spectrometer. IR spectra were obtained on a Thermo-Finnigan 370 FT-IR. Melting points of compounds were measured with a Thomas Hoover capillary melting point apparatus and are uncorrected. Elemental analyses were carried out by QTI, Whitehouse, NJ.

Electrochemical studies were carried out on either a BAS Epsilon or a CV-50W voltammetric analyzer in a three-electrode cell with a glassy carbon working electrode, a Pt wire auxiliary electrode, and a saturated calomel electrode (SCE) as the reference electrode; the latter was separated from the bulk solution by a glass frit. Steady state absorption spectra were recorded on a Hewlett-Packard diode-array spectrometer (HP 8453) with HP8453 Win System software or a Perkin-Elmer Lambda 900 spectrometer. Corrected steady-state emission measurements were conducted on a SPEX Fluoromax-2 or a Perkin-Elmer LS50B luminescence spectrometer.

The relative changes in viscosity were measured on a Cannon-Manning semi-micro viscometer. The viscometer was immersed in a constant temperature water bath (25 °C) controlled by a Neslab (model RTE-100) circulator. The irradiation source for the DNA photocleavage experiments was a 150 W Xe arc lamp in a PTI housing (Milliarc Compact Lamp Housing) powered by an LPS-220 power supply (PTI) with an LPS-221 igniter (PTI). The wavelength of the light reaching the sample was controlled by placing long-pass colored glass filters (Melles Griot) and a 10 cm water cell in the optical path. The ethidium bromide stained agarose gels were imaged using a GelDoc 2000 transilluminator (BioRad) equipped with Quality One (v. 4.0.3) software. Transient absorption spectra in the femtosecond time scale were recorded on a home-built spectrometer with a broadband detection system at 298 K as previously reported (fwhm $\approx$ 300 fs).[66]

Methods. Deoxygenated, anhydrous CH_3CN solutions containing 0.1 M tetra-*n*-butylammonium hexafluorophosphate as supporting electrolyte were used for the electrochemical measurements, and the scan rate was 100 mV/s. The oxidation potential of ferrocene (0.42 V vs SCE) was measured separately under identical experimental conditions and was used as an internal reference. Solutions used in the emission experiments were bubbled with argon for 15 min prior to each measurement. Emission quantum yields were measured in optically dilute solutions using $[Ru(bpy)_3]^{2+}$ in oxygen-free CH_3CN as the actinometer (Φ = 0.062).[67] All photophysical studies were conducted in 1 × 1 cm^2 quartz cuvettes unless otherwise noted.

The femtosecond transient absorption measurements were conducted using a Harrick Scientific flow cell (sample volume is 25 mL) equipped with CaF_2 windows, with typical sample absorbance of ~0.5 (1 mm light path length) at the excitation wavelength (~6 μJ, fwhm $\approx$ 300 fs). The transient absorption spectra were corrected for chirp in the probe continuum,[68] and the kinetic traces were analyzed by fitting to a sum of exponential terms, $S(t) = \Sigma A_i \exp(-t/\tau_i) + C$, with independent amplitudes, A_i, lifetimes, τ_i, and offset, C. Convolution with a Gaussian response function was included in the fitting procedure.

The binding constants of the metal complexes to ct-DNA determined by absorption and/or emission titrations at room temperature were measured with ~10 μM metal complex, and the ct-DNA concentration was varied from 0 to 100 μM (5 mM Tris/HCl, pH 7.5). The dilution of metal complex concentration at the end of each titration was negligible. The DNA binding constant, K_b, was obtained from fits of the titration data to eq 1,[69,70]

$$\frac{\epsilon_a - \epsilon_f}{\epsilon_b - \epsilon_f} = \frac{b - (b^2 - 2K_b^2 C_t[\mathrm{DNA}]_t/s)^{1/2}}{2K_b C_t} \quad (1)$$

where $b = 1 + K_bC_t + K_b[\mathrm{DNA}]_t/2s$, C_t and $[\mathrm{DNA}]_t$ represent the total complex and DNA concentrations, respectively, s is base pair binding site size, and ϵ_a, ϵ_f, and ϵ_b represent the molar extinction coefficients of the apparent, free, and bound metal complexes, respectively. The value of ϵ_b was determined from the plateau of the DNA titration, where addition of DNA did not result in further changes to the absorption spectrum.

DNA photocleavage experiments were carried out using 10 μL of total sample volume in 0.5 mL transparent Eppendorf tubes containing 75 μM pUC18 plasmid and 15 μM metal complex. Irradiation of the solutions was performed either in air or after 5 freeze−pump−thaw cycles in quartz tubes equipped with a Kontes stopcock (using ~3-fold greater solution volume). After irradiation, 3 μL of the DNA gel loading buffer was added to each sample (10 μL). The electrophoresis was carried out using either 1% agarose gel stained with 0.5 mg/L ethidium bromide in TAE buffer (40 mM Tris-acetate, 1 mM EDTA, pH 8.2).

The molecular and electronic structure determinations on $[Ru(tpy)_2]^{2+}$, $[Ru(tpy)(pydppz)]^{2+}$, and $[Ru(pydppz)_2]^{2+}$ were performed with density functional theory (DFT) using the Gaussian 03 (G03) program package.[71] The B3LYP[72−74] functional together with the 6-31G* basis set were used for H, C, N, and O,[75] along with the Stuttgart/Dresden (SDD) energy-consistent pseudopotentials for Ru.[76,77] All geometry optimizations were performed in C_1 symmetry with subsequent frequency analysis to show that the structures are local minima on the potential energy surface. The inclusion of solvent effects has recently been shown to be crucial when describing the electronic structure and absorption spectra of polypyridyl ruthenium complexes.[78,79] In the present work, solvent effects were modeled by single-point calculations based on the gas-phase optimized structures using the polarizable continuum model (PCM).[80,81] The orbital analysis was completed with Molekel

(66) Burdzinski, G.; Hackett, J. C.; Wang, J.; Gustafson, T. L.; Hadad, C. M.; Platz, M. S. *J. Am. Chem. Soc.* **2006**, *128*, 13402−13411.
(67) Caspar, J. V.; Meyer, T. J. *J. Am. Chem. Soc.* **1983**, *105*, 5583−5590.
(68) Nakayama, T.; Amijima, Y.; Ibuki, K.; Hamanoue, K. *Rev. Sci. Instrum.* **1997**, *68*, 4364−4371.
(69) Carter, M. T.; Rodriguez, M.; Bard, A. J. *J. Am. Chem. Soc.* **1989**, *111*, 8901−8911.
(70) Kalsbeck, W. A.; Thorp, H. H. *J. Am. Chem. Soc.* **1993**, *115*, 7146−7151.

4.3.win32.[85] The vertical singlet and triplet transition energies of the complexes were computed at the time-dependent density functional theory (TDDFT) level in CH_3CN within G03 by using the single-point calculations based on the gas-phase optimized structures for the ground state.

Results and Discussion

Synthesis. The synthesis of the target pydppz ligand started with 2-(pyrid-2′-yl)-1,10-phenanthroline (**1**), which was prepared from the Friedländer reaction of 8-amino-7-quinolinecarbaldehyde with 2-acetylpyridine.[64,86] Oxidation of **1** proceeds readily to provide the corresponding phenanthroline 5,6-quinone **2** in 78% yield (Figure 1).[87] As shown in Figure 1, the quinone can then be condensed with *o*-phenylene diamine to provide the tridentate ligand pydppz (**3**) in 98% isolated yield. The pydppz ligand was readily characterized by its ^{1}H NMR spectrum, which exhibits three well-resolved spin systems involving two, three, and four protons from the pyridylphenanthroline core. Treatment of an ethylene glycol solution of pydppz with $RuCl_3 \cdot 3H_2O$ under microwave irradiation provided the homoleptic complex $[Ru(pydppz)_2]^{2+}$, while treatment of pydppz with $[Ru(tpy)Cl_3]$ in refluxing aqueous ethanol provided the heteroleptic complex $[Ru(pydppz)(tpy)]^{2+}$.

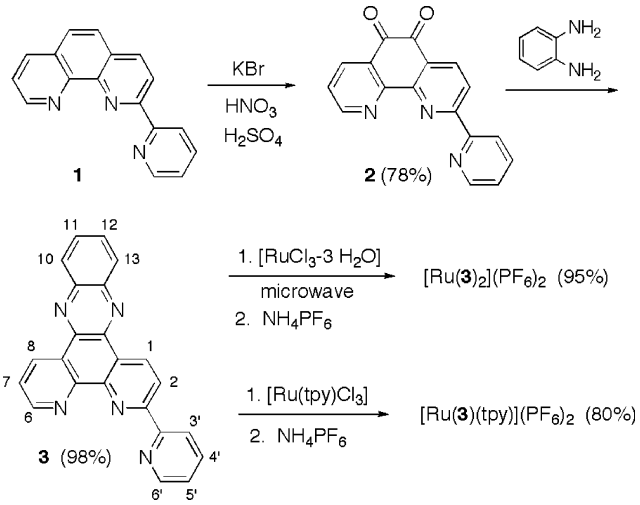

Figure 1. Preparation of pydppz (**3**) and its Ru(II) complexes.

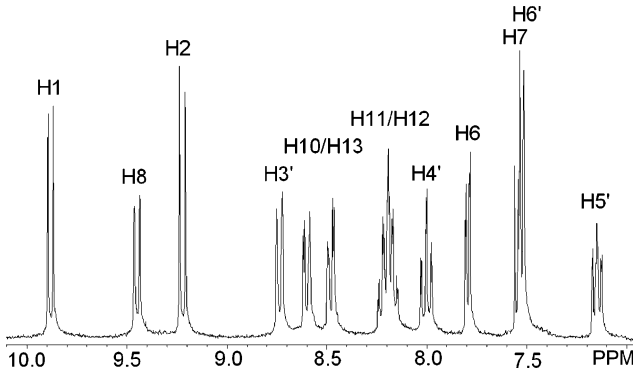

Figure 2. Downfield region of the ^{1}H NMR spectrum of $[Ru(pydppz)_2](PF_6)_2$ at 25 °C in CD_3CN. Numbering pattern from Figure 1.

Both complexes were identified by their ^{1}H NMR spectra in CD_3CN solution. The $[Ru(pydppz)_2]^{2+}$ complex possesses a C_2 symmetry axis, and therefore, the two ligands are magnetically equivalent and exhibit a single set of resonances as shown in Figure 2. There are four distinct spin systems in the molecule. Both H6 (7.79 ppm) and H6′ (7.53 ppm) show the characteristic small 5.4 Hz doublet for the three-bond coupling of a pyridine proton ortho to nitrogen. Shielding of these protons by the orthogonal ligand causes them to shift substantially upfield as compared to the uncomplexed ligand. The assignment of H3′−H5′ and H7, H8 follows through 2D connectivities (Supporting Information). The two doublets for H1 and H2 were assigned to the doublets at 9.88 and 9.22 ppm, respectively. Of the four protons on the benzo ring, H11 and H12 are nearly identical and appear as overlapping multiplets at 8.20 ppm, while H10 and H13 are deshielded by the neighboring uncomplexed nitrogen lone pairs and cannot be differentiated (8.60 and 8.48 ppm). For the heteroleptic complex $[Ru(tpy)(pydppz)]^{2+}$, the same pydppz pattern is observed superimposed on six resonances for the auxiliary tpy ligand. The integration of five of these signals corresponds to two protons each, making them readily distinguishable from the pydppz peaks.

Electronic Absorption and Emission. Figure 3 shows the absorption spectra of $[Ru(tpy)(pydppz)]^{2+}$ and $[Ru(pydppz)_2]^{2+}$ in CH_3CN, and the absorption maxima and

(71) Frisch, M. J.; Trucks, G. W.; Schlegel, H. B.; Scuseria, G. E.; Robb, M. A.; Cheeseman, J. R.; Montgomery, J. A., Jr.; Vreven, T.; Kudin, K. N.; Burant, J. C.; Millam, J. M.; Iyengar, S. S.; Tomasi, J.; Barone, V.; Mennucci, B.; Cossi, M.; Scalmani, G.; Rega, N.; Petersson, G. A.; Nakatsuji, H.; Hada, M.; Ehara, M.; Toyota, K.; Fukuda, R.; Hasegawa, J.; Ishida, M.; Nakajima, T.; Honda, Y.; Kitao, O.; Nakai, H.; Klene, M.; Li, X.; Knox, J. E.; Hratchian, H. P.; Cross, J. B.; Bakken, V.; Adamo, C.; Jaramillo, J.; Gomperts, R.; Stratmann, R. E.; Yazyev, O.; Austin, A. J.; Cammi, R.; Pomelli, C.; Ochterski, J. W.; Ayala, P. Y.; Morokuma, K.; Voth, G. A.; Salvador, P.; Dannenberg, J. J.; Zakrzewski, V. G.; Dapprich, S.; Daniels, A. D.; Strain, M. C.; Farkas, O.; Malick, D. K.; Rabuck, A. D.; Raghavachari, K.; Foresman, J. B.; Ortiz, J. V.; Cui, Q.; Baboul, A. G.; Clifford, S.; Cioslowski, J.; Stefanov, B. B.; Liu, G.; Liashenko, A.; Piskorz, P.; Komaromi, I.; Martin, R. L.; Fox, D. J.; Keith, T.; Al-Laham, M. A.; Peng, C. Y.; Nanayakkara, A.; Challacombe, M.; Gill, P. M. W.; Johnson, B.; Chen, W.; Wong, M. W.; Gonzalez, C.; Pople, J. A. *Gaussian 03*, revision C.02; Gaussian, Inc.: Wallingford, CT, 2004.
(72) Becke, A. D. *Phys. Rev. A: Gen. Phys.* **1988**, *38*, 3098.
(73) Becke, A. D. *J. Chem. Phys.* **1993**, *98*, 5648.
(74) Lee, C.; Yang, W.; Parr, R. G. *Phys. Rev. B: Condens. Matter Mater. Phys.* **1988**, *37*, 785.
(75) Hehre, W. J.; Radom, L.; Schleyer, P. v. R.; Pople, J. A. *Ab Initio Molecular Orbital Theory*; John Wiley and Sons: New York, 1986.
(76) Dolg, M.; Stoll, H.; Preuss, H. *Theor. Chim. Acta* **1993**, *85*, 441.
(77) Wedig, U.; Dolg, M.; Stoll, H. *Quantum Chemistry: The Challenge of Transition Metals and Coordination Chemistry*; Kluwer: Dordrecht, The Netherlands, 1986.
(78) Fantacci, S.; De Angelis, F.; Selloni, A. *J. Am. Chem. Soc.* **2003**, *125*, 4381−4387.
(79) De Angelis, F.; Fantacci, S.; Selloni, A. *Chem. Phys. Lett.* **2004**, 389, 204.
(80) Cances, M. T.; Mennucci, B.; Tomasi, J. *J. Chem. Phys.* **1997**, *107*, 3032.
(81) Tomasi, J.; Persico, M. *Chem. Rev.* **1994**, *94*, 2027.
(82) Cossi, M.; Barone, V.; Mennucci, B.; Tomasi, J. *Chem. Phys. Lett.* **1998**, *286*, 253.
(83) Mennucci, B.; Tomasi, J. *J. Chem. Phys.* **1997**, *106*, 5151.
(84) Cossi, M.; Scalmani, G.; Rega, N.; Barone, V. *J. Chem. Phys.* **2002**, *117*, 43.
(85) Flükiger, P.; Lüthi, H. P.; Portmann, S.; Weber, J. *MOLEKEL 4.3*: Swiss Center for Scientific Computing: Manno, Switzerland, 2000; www.cscs.ch/molekel.
(86) Riesgo, E. C.; Jin, X.; Thummel, R. P. *J. Org. Chem.* **1996**, *61*, 3017−3022.
(87) Yamada, M.; Tanaka, Y.; Yoshimoto, Y.; Kuroda, S.; Shimao, I. *Bull. Chem. Soc. Jpn.* **1992**, *65*, 1006−1011.

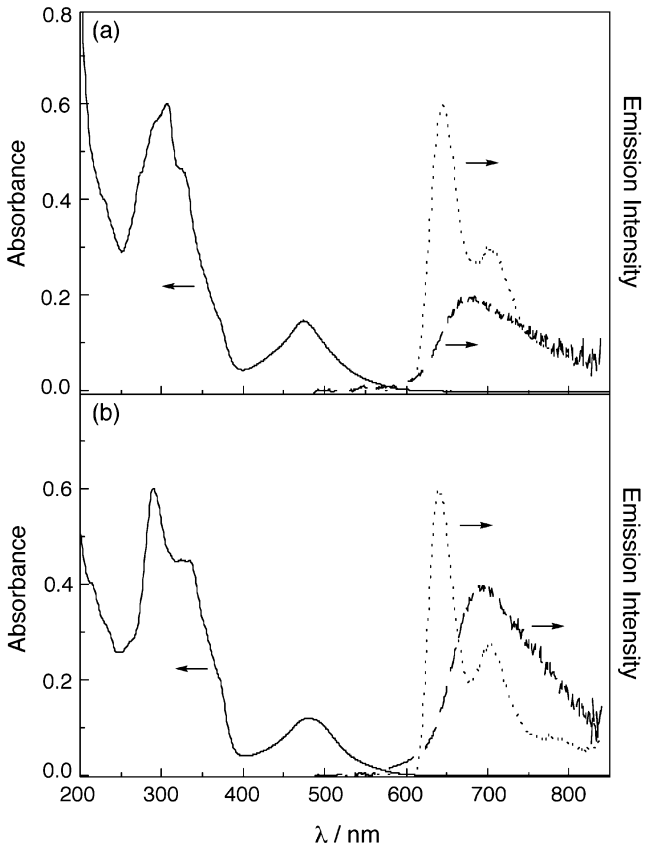

Figure 3. Electronic absorption (—) and emission spectra at 298 K (– – –, λ_{exc} = 475 nm, 10 μM) in CH_3CN and at 77 K (· · ·, λ_{exc} = 475 nm, 31 μM) in ethanol/methanol (v/v 4:1) glasses of (a) $[Ru(tpy)(pydppz)]^{2+}$ and (b) $[Ru(pydppz)_2]^{2+}$.

molar extinction coefficients of all three complexes are listed in Table 1. As is typical for Ru(II) complexes, strong absorption in the ultraviolet (UV) and near-UV regions is attributable to ligand-centered (LC) $\pi\pi^*$ transitions.[88] The tpy-centered $\pi\pi^*$ transitions in $[Ru(tpy)_2]^{2+}$ are observed at 269 and 308 nm, and $[Ru(pydppz)_2]^{2+}$ exhibits pydppz-localized $\pi\pi^*$ transitions at 291 and 327 nm (Table 1). In the heteroleptic complex $[Ru(tpy)(pydppz)]^{2+}$, $\pi\pi^*$ peaks corresponding to the superimposed transitions of the tpy and pydppz ligands are observed with maxima at 306 and 325 nm, respectively. The broad bands in the visible region observed between 475 and 481 nm in the three complexes are typical of Ru(II) complexes and correspond to $Ru(d_\pi) \rightarrow$ ligand(π^*) MLCT. The energies of these transitions are consistent with those previously reported for $[Ru(tpy)_2]^{2+}$.[89]

The emission spectra of $[Ru(tpy)(pydppz)]^{2+}$ and $[Ru(pydppz)_2]^{2+}$ at 298 K in CH_3CN and at 77 K in an ethanol/methanol (4:1) glasses are also shown in Figure 3, and Table 1 summarizes their luminescence maxima, lifetimes, and quantum yields. Both $[Ru(tpy)(pydppz)]^{2+}$ and $[Ru(pydppz)_2]^{2+}$ are weakly emissive at room temperature with maxima at 698 ($\Phi_{em} = 2.1 \times 10^{-4}$) and 678 nm ($\Phi_{em} = 6.1 \times 10^{-4}$) in CH_3CN (λ_{exc} = 475 nm), respectively. For comparison, the emission maximum of $[Ru(tpy)_2]^{2+}$ at 298 K has been previously reported at 628 nm in H_2O and at 629 nm ($\Phi_{em} \leq 5 \times 10^{-6}$) in CH_3CN.[41,89] The Stokes shifts of the emission were calculated to be 0.14 eV (1,129 cm^{-1}) for $[Ru(tpy)(pydppz)]^{2+}$ and 0.11 eV (887 cm^{-1}) for $[Ru(pydppz)_2]^{2+}$, which are typical of emissive ^{3}MLCT excited states of Ru(II) complexes.[90]

At 77 K, both complexes emit strongly with E_{00} peaks at 647 nm (1.92 eV) for $[Ru(tpy)(pydppz)]^{2+}$ and 640 nm (1.94 eV) for $[Ru(pydppz)_2]^{2+}$, showing a well-defined vibronic progression with spacing of 1312 cm^{-1} for the former and 1400 cm^{-1} for the latter (Table 1). For comparison, the vibronic spacing measured for $[Ru(tpy)_2]^{2+}$ under similar experimental conditions was 1290 cm^{-1}, which is also similar to that observed for $[Ru(bpy)_3]^{2+}$ and related complexes, and is attributed an aromatic stretching vibration of the ligands.[91] Emission lifetimes of 5.8 and 6.0 μs were measured for $[Ru(tpy)(pydppz)]^{2+}$ and $[Ru(pydppz)_2]^{2+}$, respectively, in ethanol/methanol (4:1, v/v) glasses at 77 K, while that of $[Ru(tpy)_2]^{2+}$ was measured here to be 10.8 μs and was previously reported to be 10.6 μs in butyronitrile.[41]

Electrochemistry. $[Ru(tpy)(pydppz)]^{2+}$ and $[Ru(pydppz)_2]^{2+}$ exhibit single reversible anodic waves at +1.41 and +1.42 V vs SCE in CH_3CN, respectively, that arise from the metal-centered oxidation of each complex (Table 1). These values are similar to that measured by us for the parent complex $[Ru(tpy)_2]^{2+}$, $E_{1/2}(Ru^{III/II})$ = +1.38 V vs SCE, in CH_3CN (Table 1), which is in agreement with those previously reported by others.[41,89] In addition, two well-resolved cathodic reversible waves were observed for $[Ru(tpy)(pydppz)]^{2+}$ and $[Ru(pydppz)_2]^{2+}$, while $[Ru(tpy)_2]^{2+}$ exhibits a single reduction in the experimental window at −1.21 V vs SCE in CH_3CN (Table 1), consistent with previous reports.[92] The first reduction waves in $[Ru(tpy)(pydppz)]^{2+}$ and $[Ru(pydppz)_2]^{2+}$ were measured at −0.83 and −0.86 V vs SCE (Table 1), respectively, and can be assigned as being localized on the pydppz ligand. A reduction potential of −0.88 V vs SCE was previously reported for the related complex $[Ru(bpy)_2(dppz)]^{2+}$,[93] where the reduction is localized on the dppz ligand. This similarity may indicate that in the complexes possessing the pydppz ligand, the reduction is localized on the dppz portion of the ligand. The second cathodic wave in $[Ru(tpy)(pydppz)]^{2+}$ was observed at −1.24 V vs SCE, corresponding to a tpy-centered reduction, while in $[Ru(pydppz)_2]^{2+}$ the second ligand-centered reduction was measured at −1.13 V vs SCE in CH_3CN (Table 1).

Time-Resolved Absorption. Since the ^{3}MLCT excited states of $[Ru(tpy)(pydppz)]^{2+}$ and $[Ru(pydppz)_2]^{2+}$ are short-lived at 298 K (<10 ns), transient absorption spectroscopy was conducted in the femtosecond and picosecond timescales

(88) Juris, A.; Balzani, V.; Brigelletti, F.; Campgna, S.; Belser, P.; Von, Zelewsky, A. *Coord. Chem. Rev.* **1988**, *84*, 85−277.
(89) (a) Lin, C.-T.; Böttcher, W.; Creutz, C.; Sutin, N. *J. Am. Chem. Soc.* **1976**, *98*, 6536−6544. (b) Creutz, C.; Chou, M.; Netzel, T. L.; Okumura, M.; Sutin, N. *J. Am. Chem. Soc.* **1980**, *102*, 1309−1319.
(90) Chen, P.; Meyer, T. J. *Chem. Rev.* **1998**, *98*, 1439−1477.
(91) Coe, B. J.; Thompson, D. W.; Culbertson, C. T.; Schoonover, J. R.; Meyer, T. J. *Inorg. Chem.* **1995**, *34*, 3385−3395.
(92) Bemnniston, A. C.; Grosshenny, V.; Harriman, A.; Ziessel, R. *Dalton Trans.* **2004**, 1227−1232.
(93) Bolger, J.; Gourdon, A.; Ishow, E.; Launay, J.-P. *Inorg. Chem.* **1996**, *35*, 2937−2944.

Table 1. Photophysical and Electrochemical Properties of Complexes (L = pydppz)

complex	λ_{abs}/nm ($\epsilon/\times 10^3$ M^{-1} cm^{-1})	λ_{em}/nm (Φ_{em})[a]	λ_{em}/nm (τ/μs)[b]	$E_{1/2}$/V[c]
$[Ru(tpy)_2]^{2+}$	269 (38.8), 308 (57.4), 476 (14.4)	629 ($<5.0 \times 10^{-6}$) [d]	598, 648 (10.8)[e]	+1.38, −1.21
$[Ru(tpy)(L)]^{2+}$	306 (57.2), 325 (29.6), 475 (14.8)	698 (2.1×10^{-4})	647, 707 (5.9)	+1.41, −0.83, −1.24
$[Ru(L)_2]^{2+}$	291 (90.3), 327 (64.8), 481 (18.0)	678 (8.1×10^{-5})	640, 703 (6.0)	+1.42, −0.81, −1.13

[a] In CH_3CN at 298 K. [b] At 77 K in EtOH/MeOH (4:1, v/v) glass. [c] In CH_3CN with 0.1 M Bu_4NBF_4, vs SCE. [d] From ref 41. [e] A lifetime of 10.6 μs previously reported in ref 41.

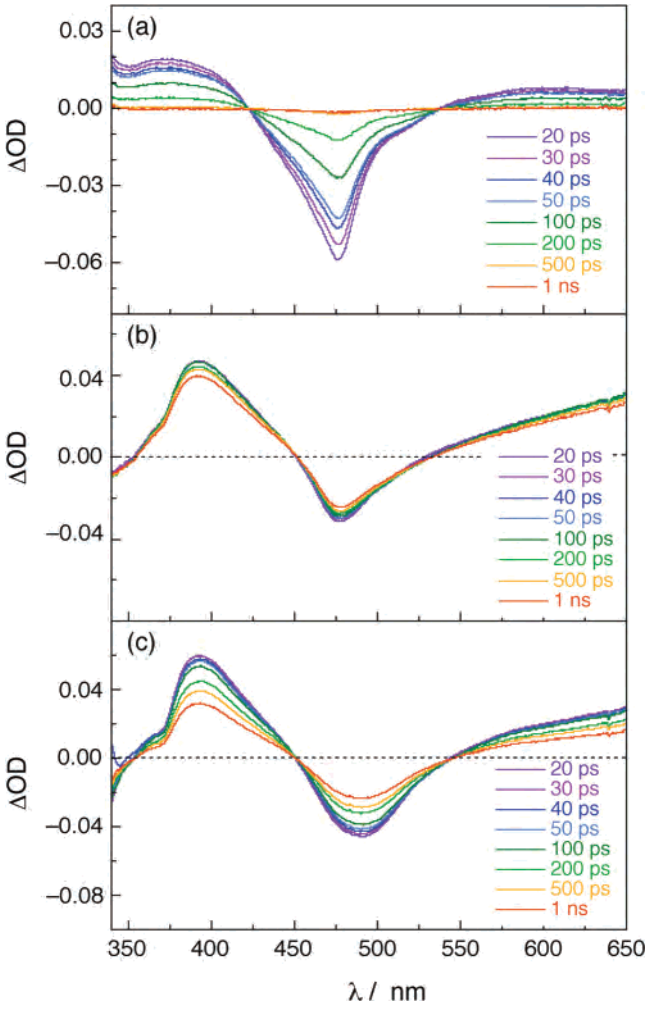

Figure 4. Transient absorption spectra of (a) 102 μM $[Ru(tpy)_2]^{2+}$, (b) 119 μM $[Ru(tpy)(pydppz)]^{2+}$, and (c) 109 μM $[Ru(pydppz)_2]^{2+}$ in CH_3CN collected at 20 ps, 30 ps, 40 ps, 50 ps, 100 ps, 200 ps, 500 ps, and 1 ns following the pump pulse (λ_{exc} = 310 nm, fwhm = 300 fs).

in order to elucidate the excited-state properties of the complexes. The difference absorption spectra of $[Ru(tpy)_2]^{2+}$, $[Ru(tpy)(pydppz)]^{2+}$, and $[Ru(pydppz)_2]^{2+}$ in CH_3CN at room temperature are shown in Figure 4 (λ_{exc} = 310 nm, fwhm ≈ 300 fs).

The transient absorption spectrum of $[Ru(tpy)_2]^{2+}$ is shown in Figure 4a and exhibits ground state bleaching from 425 to 540 nm and positive absorption features in the 350−425 nm range and at λ > 540 nm. A fast initial decay of the bleaching signal with τ < 20 ps can be assigned as arising from vibrational cooling within the ^{3}MLCT manifold,[94,95] followed by the recovery of the ground state with τ = 126(6) ps. Similar lifetimes are observed for the decay of the ^{3}MLCT signal at 370 nm, with τ = 116(6) ps. The spectral features and decay of the transient absorption spectrum of $[Ru(tpy)_2]^{2+}$ shown in Figure 4a and Supporting Information in CH_3CN are similar to those previously reported for the complex in H_2O, with a ^{3}MLCT decay lifetime of 250 ps.[96] The lifetime of the ^{3}MLCT excited state of $[Ru(tpy)_2]^{2+}$ at 298 K was also reported to be 120 ps in CH_3CN/H_2O (1:3) from transient absorption measurements,[97] and it was estimated to be 0.3 ns from its emission decay in CH_3CN ($\Phi_{em} < 1 \times 10^{-4}$).[92]

The spectral features of the transient absorption spectra of $[Ru(tpy)(pydppz)]^{2+}$ (Figure 4b) and $[Ru(pydppz)_2]^{2+}$ (Figure 4c) are qualitatively similar to those of $[Ru(tpy)_2]^{2+}$ (Figure 4a) and are characterized by a strong bleaching of the ground state absorption in the 450−550 nm range, together with intense ^{3}MLCT excited-state absorption with maxima at ∼390 nm and at λ > 550 nm (extending to the near-IR). In general, the transient absorption peaks at 390 and ∼600 nm observed in Ru(II) and Os(II) complexes have previously been ascribed as arising from the reduced tpy ligand in the ^{3}MLCT excited state.[98,99] In $[Ru(tpy)(pydppz)]^{2+}$ and $[Ru(pydppz)_2]^{2+}$, there is superposition of the bleaching due to the ground-state $\pi-\pi^*$ and the positive transient absorption signal in the 350−450 nm range, resulting negative signals at $\lambda \leq$ 375 nm. For both complexes, the lifetimes calculated from the decay of the transient absorption band at ∼390 nm and the ground state recovery from the bleaching signal at ∼480 nm are in a good agreement, indicating the two arise from the same excited state. The transient absorption spectra of $[Ru(tpy)(pydppz)]^{2+}$ and $[Ru(pydppz)_2]^{2+}$ exhibit fast initial decays after the excitation pulse from vibrational cooling (τ < 20 ps), followed by regeneration of the ground state with significantly longer lifetimes than that measured for $[Ru(tpy)_2]^{2+}$. For $[Ru(pydppz)_2]^{2+}$, fits of the signals at 392 and 480 nm result in excited-state lifetimes of 2.2 ± 0.5 and 2.4 ± 0.5 ns, respectively. Similarly, lifetimes of 5.8 ± 0.6 and 5.0 ± 0.6 ns were calculated from the decays of the signal of $[Ru(tpy)(pydppz)]^{2+}$ at 395 and 480 nm, respectively.

(94) (a) Yeh, A. T.; Shank, C. V.; McCusker, J. K. *Science* **2000**, *289*, 935−938. (b) Damrauer, N. H.; McCusker, J. K. *J. Phys. Chem. A* **1999**, *103*, 8440−8446.
(95) Bhasikuttan, A. C.; Suzuki, M.; Nakashima, S.; Okada, T. *J. Am. Chem. Soc.* **2002**, *124*, 8398−8405.
(96) Winkler, J. R.; Netzel, T. L.; Creutz, C.; Sutin, N. *J. Am. Chem. Soc.* **1987**, *109*, 2381−2392.
(97) Siemeling, U.; Vor der Brüggen, J.; Vorfeld, U.; Neumann, B.; Stammler, A.; Stammler, H.-G.; Brockhinke, A.; Plessow, R.; Zanello, P.; Laschi, F.; de Biani, F. F.; Fontani, M.; Steenken, S.; Stapper, M.; Gurzadyan, G. *Chem. Eur. J.* **2003**, *9*, 2819−2833.
(98) Lainé, P.; Bedioui, F.; Amouyal, E.; Albin, V.; Berruyer-Penaud, F. *Chem. Eur. J.* **2002**, *8*, 3162−3176.
(99) (a) Sauvage, J.-P.; Collin, J.-P.; Chambron, J.-C.; Gullerez, S.; Coudret, C.; Balzani, V.; Barigelletti, F.; De Cola, L.; Flamigni, L. *Chem. Rev.* **1994**, *94*, 993−1019. (b) Collins, J.-P.; Guillerez, S.; Sauvage, J.-P.; Barigelletti, F.; De Cola, L.; Flamigni, L.; Balzani, V. *Inorg. Chem.* **1992**, *31*, 4112−4117.

The ^{3}MLCT excited-state lifetimes of $[Ru(tpy)(pydppz)]^{2+}$ and $[Ru(pydppz)_2]^{2+}$ are ~2 orders of magnitude shorter than those of the related bpy and phen containing complexes $[Ru(bpy)_2(dppz)]^{2+}$ (740 ns) and $[Ru(phen)_2(dppz)]^{2+}$ (660 ns) in CH_3CN.[100,101] The shorter excited-state lifetime of $[Ru(tpy)_2]^{2+}$ relative to $[Ru(bpy)_3]^{2+}$ has been previously attributed to lower-lying non-emissive dd states in the former that arise from the presence of a distorted octahedral environment. The presence of these ligand field states at lower energies result in faster thermal deactivation of the emissive ^{3}MLCT state in $[Ru(tpy)_2]^{2+}$.[102] Since the structure about the metal center is expected to be similar in $[Ru(pydppz)_2]^{2+}$, $[Ru(tpy)(pydppz)]^{2+}$, and $[Ru(tpy)_2]^{2+}$, the shorter lifetime in the pydppz complexes likely arises from low-lying dd states.

The ^{3}MLCT excited-state lifetimes of the complexes decrease in the order $[Ru(tpy)(pydppz)]^{2+}$ (τ = 5.4 ns) > $[Ru(pydppz)_2]^{2+}$ (τ = 2.3 ns) > $[Ru(tpy)_2]^{2+}$ (τ = 120 ps). It has been reported that the introduction of phenyl groups in the 4, 4′, and 4″ positions of the tpy ligand in $[Ru(L)_2]^{2+}$ (L = substituted tpy) complexes increases the ^{3}MLCT excited-state lifetime by lowering the π^* orbital of the ligand, thus increasing the energy gap between the ^{3}MLCT excited state(s) and the deactivating ^{3}dd excited state(s).[37,90] From the ^{3}MLCT E_{00} energies derived from the 77 K emission maxima listed in Table 1, it is evident that the ^{3}MLCT excited states of $[Ru(tpy)(pydppz)]^{2+}$ and $[Ru(pydppz)_2]^{2+}$ lie 0.158 and 0.138 eV below that of $[Ru(tpy)_2]^{2+}$. Therefore, less deactivation of the ^{3}MLCT state of these complexes through the ^{3}dd state(s) is expected, thus resulting in longer lifetimes. The longer ^{3}MLCT lifetime of $[Ru(tpy)(pydppz)]^{2+}$ relative to that of $[Ru(pydppz)_2]^{2+}$ is also consistent with this description.

Electronic Structure Calculations. DFT calculations were performed to aid in the interpretation of the differences in the ground- and excited-state behavior of $[Ru(tpy)_2]^{2+}$, $[Ru(tpy)(pydppz)]^{2+}$, and $[Ru(pydppz)_2]^{2+}$. Figure 5a shows the relative energies of the frontier orbitals of the three complexes, all of which are characterized by three HOMOs centered on the metal, Ru(dπ), and four ligand-centered π^* LUMOs. In $[Ru(tpy)_2]^{2+}$, the four unoccupied MOs exhibit tpy(π^*) character (Figure 5a). The LUMO and LUMO+1 in $[Ru(tpy)_2]^{2+}$, where each MO is localized on one tpy ligand, correspond to the tpy-centered LUMO+3 in $[Ru(tpy)(pydppz)]^{2+}$. Similarly, the LUMO+2 and LUMO+3 orbitals in $[Ru(tpy)_2]^{2+}$ correspond to the LUMO+3 in $[Ru(tpy)(pydppz)]^{2+}$. There are two unoccupied pydppz(π^*) MOs in $[Ru(tpy)(pydppz)]^{2+}$ at lower energy, the LUMO and LUMO+1 (Figure 5a). Two nearly degenerate sets composed of these two pydppz orbitals are found in $[Ru(pydppz)_2]^{2+}$, since the two ligands in the complex are spatially separated and do not interact. The LUMO in $[Ru(tpy)(pydppz)]^{2+}$ can be correlated with the LUMO and LUMO+1 MOs in $[Ru(pydppz)_2]^{2+}$, and the LUMO+1 in the former with the LUMO+2 and LUMO+3 in the latter (Figure 5a).

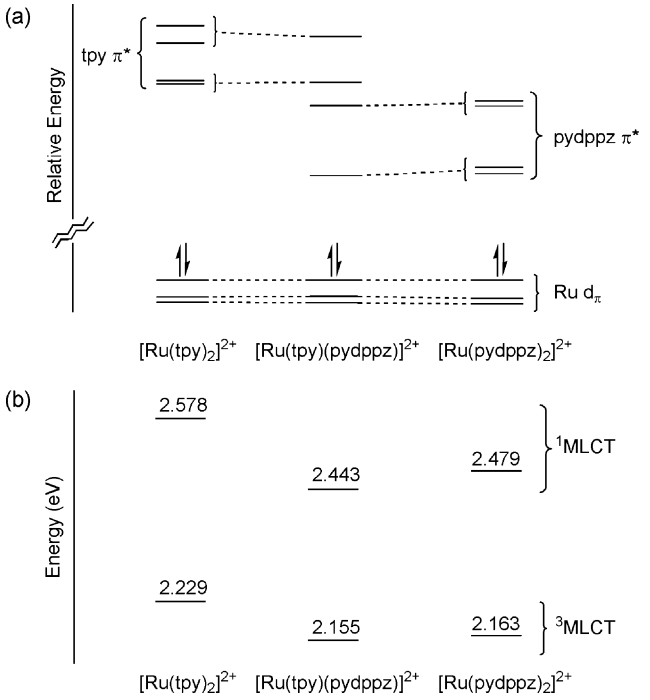

Figure 5. (a) Molecular orbital diagrams comparing the relative energies of the frontier orbitals and (b) energy comparison of the lowest energy calculated ^{1}MLCT and ^{3}MLCT states in $[Ru(tpy)_2]^{2+}$, $[Ru(tpy)(pydppz)]^{2+}$, and $[Ru(pydppz)_2]^{2+}$.

The relative energies of the LUMO calculated for the three complexes are supported by the electrochemistry. Shifts of +0.38 and +0.40 V in the reduction potential were measured for $[Ru(tpy)(pydppz)]^{2+}$ and $[Ru(pydppz)_2]^{2+}$, respectively, relative to $[Ru(tpy)_2]^{2+}$. This shift is in agreement with the calculated energy of the HOMO−LUMO gap of $[Ru(tpy)(pydppz)]^{2+}$ and $[Ru(pydppz)_2]^{2+}$ in CH_3CN, which are 0.40 and 0.39 eV smaller than that of $[Ru(tpy)_2]^{2+}$, respectively.

The absorption peaks predicted by TDDFT are consistent with the positions of the bands observed in the visible region from 400 to 600 nm for each complex. The lowest energy transition for $[Ru(tpy)_2]^{2+}$ was calculated to be ^{1}MLCT Ru(d$_\pi$) → tpy(π^*) with a maximum at 481 nm (f = 0.0128) in CH_3CN and compares well with the experimental value of 476 nm. For $[Ru(pydppz)_2]^{2+}$ the maximum of the ^{1}MLCT Ru(d$_\pi$) → pydppz(π^*) transition was calculated to be at 466 nm (f = 0.0369) in CH_3CN, with the peak observed at 481 nm in the absorption spectrum. In the heteroleptic complex, $[Ru(tpy)(pydppz)]^{2+}$, the lowest energy transition was calculated as being a combination of ^{1}MLCT transitions from Ru(d$_\pi$) to both tpy(π^*) and pydppz(π^*) at 474 (f = 0.0120) and 472 nm (f = 0.0450), respectively, consistent with the observed maximum for the complex at 475 nm in CH_3CN. A table with the calculated low-energy transitions for the three complexes can be found in the Supporting Information.

TDDFT was also used to calculate the energy and parentage of the lowest energy triplet excited states of the complexes. The calculated lowest energy triplet excited state

(100) Komatsuzaki, N.; Katoh, R.; Himeda, Y.; Sugihara, H.; Arakawa, H.; Kasuga, K. *J. Chem. Soc., Dalton Trans.* **2000**, 3053−3054.
(101) Olson, E. J. C.; Hu, D.; Hormann, A.; Jonkman, A. M.; Arkin, M. R.; Stemp, E. D. A.; Barton, J. K.; Barbara, P. F. *J. Am. Chem. Soc.* **1997**, *119*, 11458−11467.
(102) Calvert, J. M.; Caspar, J. V.; Binstead, R. A.; Westmoreland, T. D.; Meyer, T. J. *J. Am. Chem. Soc.* **1982**, *104*, 6620.

of $[Ru(tpy)_2]^{2+}$ can be ascribed as $Ru(d_\pi) \rightarrow tpy(\pi^*)$ ^{3}MLCT with a vertical energy of 2.23 eV (556 nm) from the minimized singlet ground state. As shown in Figure 5b, the ^{3}MLCT excited state lies 0.35 eV below the lowest energy ^{1}MLCT state in $[Ru(tpy)_2]^{2+}$. The calculated vertical energy of the ^{3}MLCT state is 0.16 eV greater than the E_{00} value of 2.07 eV (598 nm, Table 1) obtained from the low-temperature emission for the complex. The difference in the two values can be explained by the change in equilibrium nuclear positions between the ground state and the excited state, since the emission takes place from the thermally equilibrated ^{3}MLCT state. Similarly, the calculations are consistent with the lowest energy triplet states of $[Ru(tpy)(pydppz)]^{2+}$ and $[Ru(pydppz)_2]^{2+}$ arising from $Ru(d_\pi) \rightarrow pydppz(\pi^*)$ ^{3}MLCT, with vertical energies of 2.155 (575 nm) and 2.163 eV (573 nm), respectively. For these complexes E_{00} energy determined from the emission maxima at 77 K were measured at 647 nm (1.916 eV) in the former and at 640 nm (1.937 eV) in the latter (Table 1), such that the calculated ^{3}MLCT energies for these complexes are ~0.22 eV greater than the experimental E_{00} values. Although the absolute energies of the states are shifted relative to the experimental values by ~0.2 eV in all complexes, relative comparisons can still be made. The calculated energies of the lowest energy ^{3}MLCT excited states of $[Ru(pydppz)_2]^{2+}$ and $[Ru(tpy)(pydppz)]^{2+}$ lie 0.067 and 0.074 eV lower in energy than that of $[Ru(tpy)_2]^{2+}$. This trend is consistent with the experimental findings at 77 K, where the difference was found to be ~0.07 eV.

DNA Binding and Emission Enhancement with DNA. Unlike $[Ru(tpy)_2]^{2+}$, hypochromic and bathochromic shifts are observed in the absorption spectra of $[Ru(tpy)(pydppz)]^{2+}$ and $[Ru(pydppz)_2]^{2+}$ in the presence of DNA. The changes to the absorption spectrum of 12.5 μM $[Ru(tpy)(pydppz)]^{2+}$ upon addition of up to 74 μM DNA (5 mM Tris, pH 7.4, 50 mM NaCl) result in hypochromic shifts of 23% and 24% measured at 300 and 475 nm, respectively, with a modest (~4 nm) bathochromic shift (Supporting Information). Similarly, 14% and 13% hypochromicity was observed at 335 and 480 nm, respectively, for 9.0 μM $[Ru(pydppz)_2]^{2+}$ upon addition of 57 μM DNA. The DNA binding constants, K_b, of $[Ru(tpy)(pydppz)]^{2+}$ and $Ru(pydppz)_2]^{2+}$ were calculated to be 2.0×10^6 M^{-1} ($s = 1.23$) and 8.1×10^6 M^{-1} ($s = 1.07$), respectively, from fits of the absorption changes as a function of [DNA] for each complex (Supporting Information). Absorption titrations resulted in similar values of K_b for the DNA intercalating complexes $[Ru(phen)_2(dppz)]^{2+}$ ($1 \times 10^6 - 5 \times 10^6$ M^{-1}; phen = 1,10-phenanthroline)[103,104] and $[Ru(bpy)_2(tpphz)]^{2+}$ (5.1×10^6 M^{-1}).[24]

The DNA intercalation of $[Ru(tpy)(pydppz)]^{2+}$ was confirmed using relative viscosity measurements.[47,48] Figure 6a illustrates the increase in the relative viscosity of 1 mM herring sperm DNA upon addition of the known intercalator ethidium bromide (EtBr) and $[Ru(tpy)(pydppz)]^{2+}$. These

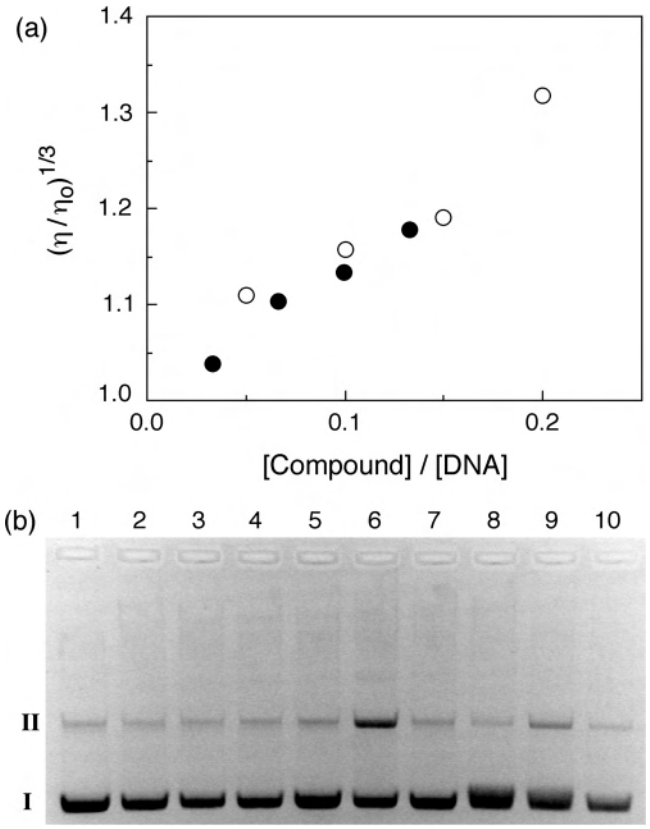

Figure 6. (a) Changes in the relative viscosity of solutions containing 1 mM herring sperm DNA (5 mM Tris, 50 mM NaCl, pH 7.4) as a function of the concentration of ethidium bromide (O) and $[Ru(tpy)(pydppz)]^{2+}$ (●). (b) Ethidium bromide imaged agarose gel with 75 μM pUC18 plasmid (all lanes) and 15 μM $[Ru(tpy)_2]^{2+}$ (lanes 2−4), 15 μM $[Ru(tpy)(pydppz)]^{2+}$ (lanes 5−7), or 15 μM $[Ru(pydppz)_2]^{2+}$ (lanes 8−10) in 5 mM Tris, pH 7.5, 50 mM NaCl. Lane 1: plasmid only, dark; lanes 2, 5, and 8: dark; lanes 3, 6, and 9: irradiated in air; lanes 4, 7, and 10: irradiated after freeze−pump−thaw ($\lambda_{irr} \geq 395$ nm, 10 min).

changes are consistent with intercalation by the complex between the DNA bases. Owing to the large concentrations required for the relative viscosity measurements and the low solubility of $[Ru(pydppz)_2]^{2+}$ in water, this measurement was not possible for this complex. Since both $[Ru(tpy)(pydppz)]^{2+}$ and $[Ru(pydppz)_2]^{2+}$ possess the intercalating pydppz ligand and exhibit hypochromic and bathochromic shifts upon addition of DNA, it is believed that latter also binds to DNA through intercalation.

As is typical of other Ru(II) complexes with ligands that intercalate between the DNA bases, the emission intensity of 12.5 μM $[Ru(tpy)(pydppz)]^{2+}$ is enhanced 8-fold upon the addition of 74 μM ct-DNA in 5 mM Tris, pH 7.5, 50 mM NaCl (Supporting Information), with a shift in the maximum from 729 to 699 nm. In contrast, the luminescence of 9.0 μM $[Ru(pydppz)_2]^{2+}$ only increases by a factor of 1.2 as DNA is added up to 57 μM. For both complexes, further increase in the DNA concentration did not result in additional changes to the emission intensity.

A possible explanation for these observations is that only one pydppz ligand of $[Ru(pydppz)_2]^{2+}$ intercalates into DNA base-pair stack, while the other remains exposed to the buffer. It has been proposed that in "DNA light-switch" complexes, such as $[Ru(bpy)_2(dppz)]^{2+}$, the emissive (bright) excited

(103) Haq, I.; Lincoln, P.; Suh, D.; Norden, B.; Chowdhry, B. Z.; Chaires, J. B. *J. Am. Chem. Soc.* **1995**, *117*, 4788−4796.
(104) Nair, R. B.; Teng, E. S.; Kirkland, S. L.; Murphy, C. J. *Inorg. Chem.* **1998**, *37*, 139−141.

state lies above a non-emissive (dark) state in energy and that the energy difference between these states is dependent on the surrounding medium and results in the variation of the luminescence intensity.[105] It is believed that in aqueous media the energy difference between the bright and dark states is large, such that thermal population of the former cannot take place at room temperature.[105] Upon DNA intercalation of the ligand, however, the energy of the dark state increases such that the emissive state is thermally accessible, thus resulting in luminescence enhancement.[105] A similar mechanism is likely operative in the emission enhancement of $[Ru(tpy)(pydppz)]^{2+}$ observed upon DNA intercalation of the pydppz ligand, where the dark state in the complex is raised in energy. In contrast, two dark states and two bright states are expected in $[Ru(pydppz)_2]^{2+}$, since it possesses two ligands with an extended π-system. Owing to the disposition of the two intercalating ligands in $[Ru(pydppz)_2]^{2+}$, only one pydppz ligand can intercalate in a DNA duplex, leaving the other ligand exposed to the solvent. If this is the case, then the energy of the dark state associated with the non-intercalated ligand will remain too low to permit population of the bright state at room temperature, resulting in no emission enhancement for this complex in the presence of DNA.

DNA Photocleavage. The imaged ethidium bromide stained agarose gel in Figure 6b shows the DNA photocleavage by $[Ru(tpy)(pydppz)]^{2+}$ upon irradiation with visible light. Lane 1 shows that 75 μM pUC18 plasmid alone is found mostly supercoiled (Form I), with a small amount of nicked plasmid (Form II). It is evident from Figure 6b that no DNA damage occurs in the presence of 15 μM $[Ru(tpy)_2]^{2+}$ in the dark or irradiated ($\lambda_{irr} > 395$ nm, 10 min) in air or in the absence of O_2 (Lanes 2−4). Similarly, no DNA cleavage is observed when the plasmid is exposed to 15 μM $[Ru(tpy)(pydppz)]^{2+}$ or 15 μM $[Ru(pydppz)_2]^{2+}$ in the dark (Lanes 5 and 8), however, irradiation of 75 μM pUC18 in the presence of 15 μM $[Ru(tpy)(pydppz)]^{2+}$ ($\lambda_{irr} > 395$ nm, 10 min) in air (Lane 6) results in single-stranded cleavage with the production of nicked plasmid (Form II). In contrast, DNA cleavage by 15 μM $[Ru(tpy)(pydppz)]^{2+}$ is not apparent when the sample is irradiated in the absence of O_2 (Lane 7). Unlike the heteroleptic complex, no DNA damage is observed upon irradiation of plasmid with visible light ($\lambda_{irr} > 395$ nm, 10 min) in the presence of 15 μM $[Ru(pydppz)_2]^{2+}$ in air (Lane 9) or in the absence of O_2 (Lane 10).

These results indicate that the mechanism of DNA photocleavage by $[Ru(tpy)(pydppz)]^{2+}$ is mediated by oxygen, likely through the sensitized production of $^1O_2$, as is typical of polypyridyl Ru(II) complexes.[31,106,107] Of the three complexes, the lifetime of $[Ru(tpy)(pydppz)]^{2+}$ is the longest, and this complex is the only one of the series that exhibits emission enhancement in the presence of DNA. Although the excited-state lifetime of $[Ru(tpy)(pydppz)]^{2+}$ is short (~5 ns) in CH_3CN, the small amount of $^1O_2$ produced appears to be enough for DNA damage to be observed, owing to the extremely high sensitivity of the technique. Similar results were previously reported for related Ru(II) complexes possessing modified tpy ligands with short excited-state lifetimes.[35]

The quantum yield of the production of $^1O_2$ generated through photosensitization by the complexes was measured using $[Ru(bpy)_3]^{2+}$ as a standard ($\Phi_{1O2} = 0.81$ in CH_3OH)[108] and 1,3-diphenyl-isobenzofuran as a reactant with known spectroscopic features.[35,109] The quantum yields of $^1O_2$ produced upon irradiation ($\lambda = 475$ nm) of $[Ru(tpy)_2]^{2+}$ and $[Ru(pydppz)_2]^{2+}$ in CH_3OH were 1.0(4)% and 0.9(4)%, respectively. In contrast, a 2-fold greater quantum yield, 1.9(3)%, was observed for $[Ru(tpy)(pydppz)]^{2+}$. The greater production of photosensitized $^1O_2$ by the heteroleptic complex is consistent with its longer ^{3}MLCT lifetime.

Conclusions

The ligand pydppz, a tridentate analogue of dppz having a 2′-pyridyl group appended at the 3-position, has been synthesized in two simple steps from 2-(pyrid-2′-yl)-1,10-phenanthroline. Homo- and heteroleptic complexes, $[Ru(pydppz)_2]^{2+}$and $[Ru(tpy)(pydppz)]^{2+}$, were prepared and characterized by ^{1}H NMR. The absorption and emission spectra are consistent with low-lying MLCT excited states, which are typical of Ru(II) complexes. Femtosecond transient absorption measurements show that that the heteroleptic complex $[Ru(tpy)(pydppz)]^{2+}$ ($\tau \approx 5$ ns) is longer-lived than $[Ru(pydppz)_2]^{2+}$ ($\tau = 2.4$ ns) and that the lifetime of both complexes is significantly longer than that of the parent complex $[Ru(tpy)_2]^{2+}$ ($\tau = 120$ ps). These differences are explained by the lower energy ^{3}MLCT excited state present in $[Ru(tpy)(pydppz)]^{2+}$ and $[Ru(pydppz)_2]^{2+}$ compared to $[Ru(tpy)_2]^{2+}$, thus resulting in less deactivation of the former through the ligand-field state(s). DFT and TDDFT calculations are consistent with this explanation.

$[Ru(tpy)(pydppz)]^{2+}$ and $[Ru(pydppz)_2]^{2+}$ bind to DNA through the intercalation of the pydppz ligand; however, only the heteroleptic complex exhibits luminescence enhancement in the presence of the double helix. The difference in the photophysical behavior of the complexes is explained by the inability of $[Ru(pydppz)_2]^{2+}$ to intercalate both pydppz ligands; thus, one pydppz remains exposed to the solvent. DNA photocleavage is observed for $[Ru(tpy)(pydppz)]^{2+}$ in air, but not for $[Ru(pydppz)_2]^{2+}$. The DNA damage likely proceeds through the production of small amounts of $^1O_2$ sensitized by the excited state of the longer-lived complex. Although both complexes possess the intercalating pydppz

(105) (a) Pourtois, G.; Beljonne, D.; Moucheron, C.; Schumm, S.; Mesmaeker, A. K.-D.; Lazzaroni, R.; Bredas, J.-L. *J. Am. Chem. Soc.* **2004**, *126*, 683. (b) Brennaman, M. K.; Meyer, T. J.; Papanikolas, J. M. *J. Phys. Chem. A* **2004**, *108*, 9938. (c) Brennaman, M. K.; Alstrum-Acevedo, J. H.; Fleming, C. N.; Jang, P.; Meyer, T. J.; Papanikolas, J. M. *J. Am. Chem. Soc.* **2002**, *124*, 15094.

(106) Hergueta-Bravo, A.; Jimenez-Hernandez, M. E.; Montero, F.; Oliveros, E.; Orellana, G. *J. Phys. Chem. B* **2002**, *106*, 4010−4017.

(107) (a) Chouai, L.; Wicke, S.; Turro, C.; Bacsa, J.; Dunbar, K. R.; Thummel, R. P. *Inorg. Chem.* **2005**, *44*, 5996−6003. (b) Fu, P. K.-L.; Bradley, P. M.; van Loyen, D.; Dürr, H.; Bossmann, S. H.; Turro, C. *Inorg. Chem.* **2002**, *41*, 3808−3810.

(108) Bhattacharyya, K.; Das, P. K. *Chem. Phys. Lett.* **1985**, *116*, 326.

(109) Young, R. H.; Wehrly, K.; Martin, R. L. *J. Am. Chem. Soc.* **1971**, *93*, 5774.

ligand, they exhibit different photophysical properties in the presence of DNA.

Acknowledgment. C.T. thanks the NSF (CHE 0503666), Ohio Supercomputer Center, and CCBD for their generous support. R.P.T. thanks the Robert A. Welch Foundation (E-621) and the National Science Foundation (CHE-0352617) for financial support. D.A.L. thanks The Ohio State University for a Presidential Fellowship.

Supporting Information Available: DNA titration, transient absorption decays, 2D NMRs, TDDFT calculated singlet and triplet transition energies, and low-lying unoccupied MOs. This material is available free of charge via the Internet at http://pubs.acs.org.

IC700484J